



HAL
open science

Synthesis of Furfuryl Alcohol from Furfural: A Comparison between Batch and Continuous Flow Reactors

Maité Audemar, Yantao Wang, Deyang Zhao, Sébastien Royer, François Jerome, Christophe Len, Karine de Oliveira Vigier

► **To cite this version:**

Maité Audemar, Yantao Wang, Deyang Zhao, Sébastien Royer, François Jerome, et al.. Synthesis of Furfuryl Alcohol from Furfural: A Comparison between Batch and Continuous Flow Reactors. *Energies*, 2020, 13 (4), pp.1002. 10.3390/en13041002 . hal-03015037

HAL Id: hal-03015037

<https://hal.science/hal-03015037v1>

Submitted on 19 Nov 2020

HAL is a multi-disciplinary open access archive for the deposit and dissemination of scientific research documents, whether they are published or not. The documents may come from teaching and research institutions in France or abroad, or from public or private research centers.

L'archive ouverte pluridisciplinaire **HAL**, est destinée au dépôt et à la diffusion de documents scientifiques de niveau recherche, publiés ou non, émanant des établissements d'enseignement et de recherche français ou étrangers, des laboratoires publics ou privés.

1 Communication

2 Synthesis of furfuryl alcohol from furfural: a 3 comparison between batch and continuous flow 4 reactors

5 Maïté Audemar ¹, Yantao Wang ^{2,3}, Deyang Zhao ^{2,4}, Sébastien Royer,⁵ François Jérôme,¹
6 Christophe Len ^{2,4} and Karine De Oliveira Vigier ^{1,*}

7 ¹ Université de Poitiers, IC2MP, UMR CNRS 7285, 1 rue Marcel Doré, 86073 Poitiers Cedex 9;

8 karine.vigier@univ-poitiers.fr

9 ² Sorbonne universités, Université de Technologie de Compiègne, Centre de recherche Royallieu, CS 60 319,

10 F-60203 Compiègne cedex, France

11 ³ School of Resources Environmental & Chemical Engineering, Nanchang university, Nanchang,

12 330031, China.

13 ⁴ ChimieParisTech, PSL Research University, CNRS, Institute of Chemistry for Life and Health Sciences, 11

14 rue Pierre et Marie Curie, F-75005 Paris, France; christophe.len@chimieparistech.psl.eu

15 ⁵ Univ. Lille, CNRS, ENSCL, Centrale Lille, Univ. Artois, UMR 8181 - UCCS - Unité de Catalyse et de Chimie
16 du Solide, F-59000 Lille, France, E-mail: sebastien.royer@univ-lille.fr

17 * Correspondence: karine.vigier@univ-poitiers.fr

18 Received: date; Accepted: date; Published: date

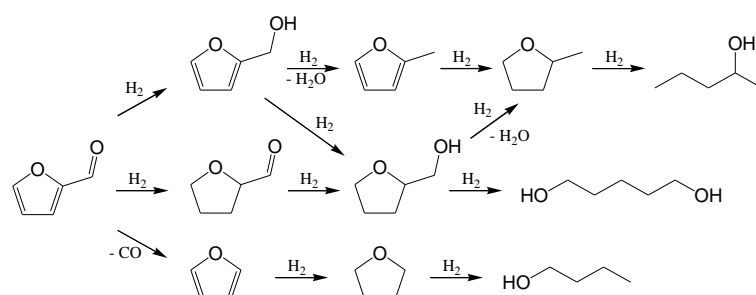
19 **Abstract:** Furfural is a platform molecule obtained from hemicellulose. Among the products that
20 can be produced from furfural, furfuryl alcohol is one of the most studied. It is synthesized at an
21 industrial scale in the presence of CuCr catalyst but this process suffers from an environmental
22 negative impact. Here, we demonstrate that a non-noble metal catalyst (Co/SiO₂) was active (100%
23 conversion of furfural) and selective (100% selectivity to furfuryl alcohol) in the hydrogenation of
24 furfural to furfuryl alcohol at 150°C under 20 bar of hydrogen. This catalyst was recyclable up to 3
25 cycles and then the activity decreased. Thus, a comparison between batch and continuous flow
26 reactor shows that changing the reactor type helps to increase the stability of the catalyst and the
27 space-time yield. This study shows that continuous flow reactor can be a solution when a catalyst
28 suffered from a lack of stability in batch process.

29 **Keywords:** Continuous flow; batch reactor; furfural; furfuryl alcohol; hydrogenation.

30

31 1. Introduction

32 Motor fuels components and fine chemicals can be produced from non-edible plant-based
33 feedstocks using catalytic processes. Among all the available starting materials, furfural is one of the
34 most promising compounds, as it is a platform molecule for the synthesis of a high number of
35 chemicals for a wide range of applications [1–4]. Furfural production is based on acid hydrolysis of
36 hemicellulose [5]. One interesting reaction from furfural is hydrogenation reaction that is the most
37 significant process in the furfural conversion. The hydrogenation of furfural leads to the production
38 of valuable chemicals such as furfuryl alcohol (FOL), 2-methylfuran (2-MF), tetrahydrofurfuryl
39 alcohol (THFA), etc. Currently, around 50% of the furfural production is employed for the synthesis
40 of furfuryl alcohol (FA) which can be used for resins, flavors, as components of motor fuels (alkyl
41 levulinates) and in the pharmaceutical industry (ranitidine), biochemistry, etc. During the
42 hydrogenation of furfural to FOL many side reactions can occur such as the formation of THFA, 2-
43 methylfurane, etc (Scheme 1). The precise control of the selectivity of the reaction by using an
44 appropriate and stable catalyst is highly demanded.

45
4647
48
49
50

Scheme 1. Hydrogenation of furfural.

51 Copper-chromium (CuCr) alloy is the catalyst used on industrial scale to produce FOL with a
 52 high yield (98%) [5]. This catalyst has some drawbacks such as the presence of chromium which can
 53 contaminate FOL and hampers its use in pharmaceutical industry for instance. Moreover chromium-
 54 containing catalysts can be deactivated due to shielding of copper by chromium [6]. Many researches
 55 were devoted to the replacement of this catalyst by catalysts based on noble metals such as Pt and Pd
 56 [7-11], leading to an increase of the process cost. Furthermore, FOL selectivity is lower in the presence
 57 of these catalysts than in the presence of chromium–copper systems. To increase the selectivity to
 58 FOL, the addition of metals such as Cu to Pd based catalysts results in the improvement of the
 59 selectivity to FOL (98% of FOL was obtained) [12]. Non-noble metals catalysts were also studied in
 60 the selective hydrogenation of furfural to FOL such as supported Ni, Cu, Fe, Mo, Zn, etc. [13–18].
 61 Various methods were used for the synthesis of catalysts, additives, process conditions, and various
 62 solvents in the case of a liquid phase process [19–21]. Several drawbacks are present using this system:
 63 deactivation due to the sintering of active species; poisoning of the catalyst surface by coke formation;
 64 low selectivity of FOL; high temperature and pressure. Up to now, several studies of selective
 65 hydrogenation of furfural to FOL are performed in the liquid phase in batch reactors using different
 66 solvents, but very little attention is paid to the process in a flow system [22–26]. To this aim,
 67 hydrogenation of furfural to FOL was studied in the presence of Co/SiO₂ catalyst in batch and in
 68 continuous flow reactors. We demonstrate here that despite the high selectivity and activity of the
 69 Co/SiO₂ catalyst in the hydrogenation of furfural in batch reactor, the reaction performed in a
 70 continuous flow reactor led to a higher space time yield (STY=quantity of FOL produced per unit
 71 volume unit per time unit). STY was three times higher when the hydrogenation of furfural is
 72 performed in a continuous flow reactor than in a batch process. The selectivity was slightly lower in
 73 continuous flow reactor than in bath reactor but the activity was similar. The catalyst was more stable
 74 under flow reactor than in batch reactor.

75

76 2. Materials and Methods

77 *Catalyst preparation:* The Co₃O₄/SiO₂ material, with a metal loading of 10 wt.% is prepared using
 78 incipient wetness impregnation method as described previously [27] using Co(NO₃)₂ and aerosil
 79 silica (380). The dry solid is calcined at 500 °C for 6 h to obtain the Co₂O₃/SiO₂ sample. Co₂O₃/SiO₂
 80 (around 100 mg) is reduced under hydrogen flow (3 L.h⁻¹) at 500 °C for 10 h.

81

82 *Catalyst characterizations:* Co/SiO₂ catalyst was characterized by ICP-OES, XRD analysis, N₂-
 83 physisorption, Transmission Electronic Microscopy, Thermal analysis. Perkin Elmer Optima 2000 DV
 84 instrument is used for ICP analysis. The catalysts was first dissolved in a mixture of HF and HCl
 85 under micro-wave for digestion before analysis. XRD analysis is performed using a Bruker Empyrean
 86 with a Co cathode. N₂-physisorption experiments were obtained on an Autosorb 1-MP instrument,
 87 at 77K. The catalysts are treated under vacuum à 350 °C for 3 h and the surface area, the pore size as
 88 well as the pore volume are determined as described previously [27]. TEM experiments are

89 performed on a JEOL 2100 UHR instrument operated at 200 kV, equipped with a LaB6 source and a
90 Gatan ultra scan camera. Thermal analysis are performed using a TA instrument (SDTQ 600) under
91 air flow of 100 mL·min⁻¹ from 25 °C to 800 °C.

92

93 *General procedure for the hydrogenation of furfural in a batch reactor:* in a typical experiment, 1 g of
94 furfural is added to 9 g of ethanol and 50 mg of catalyst is added in a batch reactor (75 mL). The
95 hydrogen pressure is fixed to the desired one. Then, the temperature is increased up to the desired
96 reaction temperature *i.e.* 150 °C. At the end of the reaction, the reactor is cooled down to room
97 temperature, and liquid phase is analysed.

98

99 *General procedure for the hydrogenation of furfural in flow reactor:* The experiments were carried
100 out in H-Cube Pro™ Flow Reactor ThalesNano™, Hungary, connected to a HPLC pump to supply
101 a continuous feed of 10 wt% furfural in ethanol. A 70 mm catalyst cartridge (0.88 mL empty volume)
102 catalyst was packed with 260 mg catalyst by applying vacuum suction at the bottom of the cartridge.
103 The total flow through volume (including feed, reactor and product sections) was 6 mL. First, pure
104 ethanol was pumped through the system and then the feed was changed to the furfural-ethanol
105 mixture. The flow was continued until the desired temperature and hydrodynamic pressurization
106 (20–60 bar) of the reactor module were reached. Depending on the flow rate used (0.2–0.5 mL min⁻¹),
107 the reaction time was set (20–50 min) before collecting the first sample (time zero). The samples were
108 collected after regular time intervals.

109 *Analytical methods :* yields to furfuryl alcohol and conversion of furfural are determined by
110 external calibration at 25 °C by HPLC equipped with a nucleosil 100–5 C18 column (250 mm and
111 diameter of 4.6 mm), a Shimadzu LC-20AT pump, and a Shimadzu RID-10 A detector using
112 acetonitrile/water (10:90) as the mobile phase (0.6 mL·min⁻¹).

113 Continuous flow results were detected on a gas chromatograph (HP, 14009 Arcade, New York,
114 United States) coupled with a FID detector equipped with a Supelco 2-8047-U capillary column (15
115 m x 0.25 mm i.d. and 0.25 µm film thickness, Alltech Part No.31163-01). The flow rate of the carrier
116 gas (H₂) was 1 mL min⁻¹. The injector temperature was 250 °C and the oven started at 70 °C for 1 min,
117 and the temperature was increased up to 250 °C at a rate of 20 °C min⁻¹, and the temperature was
118 then maintained at 250 °C for 10 min.

119

120 3.1. Catalyst characterization

121 The catalyst was prepared using Incipient Wetness Impregnation (IWI) method. After calcination
122 of the solid at 500 °C under air, oxide precursor, Co₃O₄/SiO₂, is obtained, confirmed by XRD analysis
123 (Figure 1(a)), with the presence of peaks corresponding to the awaited position (PDF file 01-1152).
124 Considering the width of the reflections, the cobalt crystal size is relatively low (<10 nm). This result
125 confirms that using this impregnation method, high dispersion of the cobalt oxide phase was
126 achieved. The loading of cobalt was evaluated by ICP-OES and was of 9 wt. %

127

128

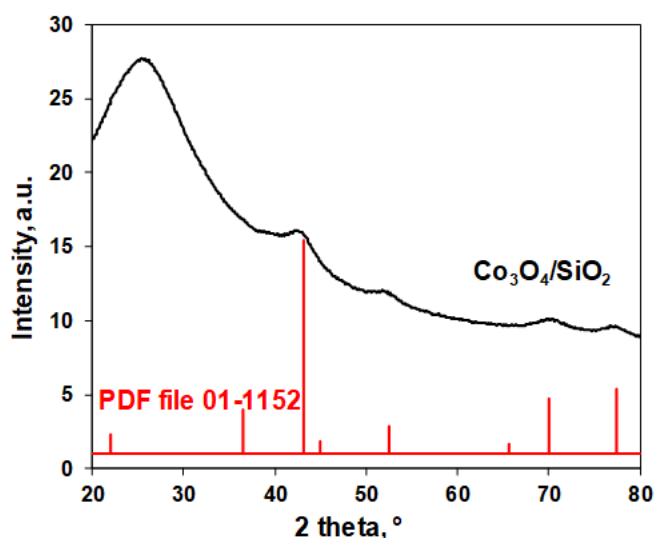


Figure 1. XRD analysis of non reduced Co/SiO₂ catalyst (vertical bars, Co₃O₄ reference PDF file 01-1152).

The catalyst is reduced under H₂ flow at 500°C for 10h prior to catalytic test leading to a large surface area and large pore diameter, suitable for liquid phase hydrogenation reaction. Moreover, the limited evolution of the textural properties indicates adequate stabilities of the support (Table 1).

Table 1. Main characteristics of the Co₃O₄/SiO₂ and reduced Co/SiO₂ materials

	Co ₃ O ₄ /SiO ₂	Co/SiO ₂
XRD phase	Poorly crystallized Co ₃ O ₄	n.d. ^[a]
Dpart./b nm	n. d. ^[a]	Aggregates 10 to >100 nm Crystals <20 nm
SBET/c m ² .g ⁻¹	185	169
Vp/ cm ³ .g ⁻¹	0.71	0.63
Dp/ nm	15.0	14.7

¹ [a] n.d.: not determined; [b] mean particle size obtained by TEM image observation; [c] surface area (S_{BET}), pore volume (V_p) and pore diameter (D_p) issued from N₂ physisorption at 77K.

Figure 2 shows that the particle sizes and localization throughout the support porosity are not homogeneous and aggregates of NPs of cobalt are observed throughout the surface of the silica with a size of 20-100 nm. Energy Dispersive X-Ray Spectroscopy (EDS) showed that dark mark are cobalt particle and hexagonal cobalt phase was observed using electron diffraction.

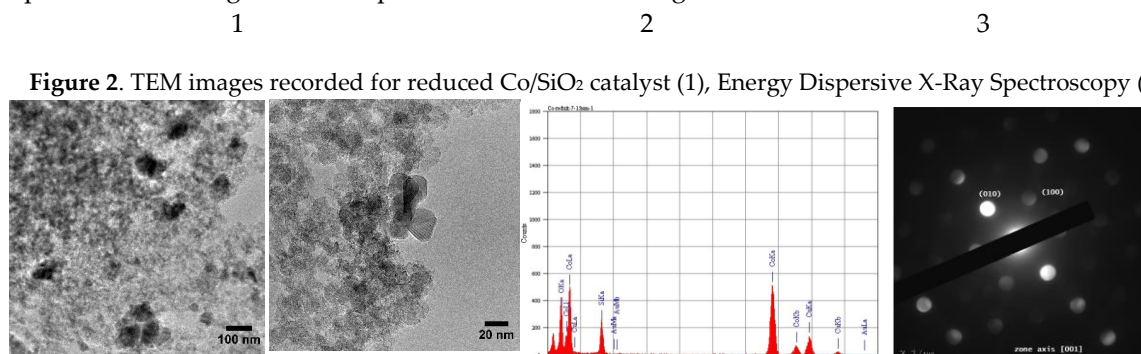


Figure 2. TEM images recorded for reduced Co/SiO₂ catalyst (1), Energy Dispersive X-Ray Spectroscopy (EDS)

(2) and electron diffraction analysis (3).

3.2. Hydrogenation of furfural in batch reactor.

147 The hydrogenation of furfural was performed in a batch reactor starting from 1g of furfural in
 148 9g of ethanol in the presence of 50 mg of catalyst (Table 2).

149 **Table 2.** Hydrogenation of furfural in a batch reactor¹.

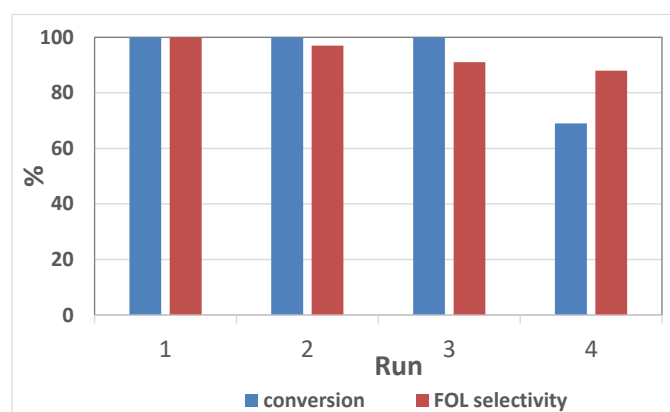
	Reaction time (h)	P _{H2} (bar)	Temperature (°C)	Conversion (%)	Selectivity to FOL (%)	STY (g.L ⁻¹ .h ⁻¹)
entry 1	1	20	150	100	100	13.2
entry 2	1,5	20	150	100	65	5.9
entry 3	1	40	150	100	85	11,4
entry 4	1	20	180	100	80	10,8

150 ¹ Furfural = 1g, ethanol = 9g, Co/SiO₂ = 50 mg

151 We were pleased to see that furfural conversion reached 100% at 150°C after 1h of reaction, with
 152 a FOL yield of 100% (Table 2, entry 1). By prolonging the reaction time, the yield of FOL decreased
 153 from 100% to 65% due to further hydrogenation of FOL to THFA (Table 2, entry 2). This result shows
 154 that Co/SiO₂ was active and selective in the hydrogenation of furfural to FOL. An increase of
 155 hydrogen pressure led to a decrease of FOL yield due to the further hydrogenation of FOL to THFA
 156 that can be favored by a higher solubility of hydrogen than at lower pressure of hydrogen (Table 2,
 157 entry 3). In both conditions, FOL is further hydrogenated to THFA. A similar trend was observed
 158 with an increase of the temperature from 150 to 180°C. With the increase of the temperature, THFA
 159 was also observed as a by-product and the selectivity of FOL decreased on the benefit of the formation
 160 of THFA. Based on these results, it is of prime importance to control the kinetic of the reaction in
 161 order to prevent further hydrogenation of FOL to THFA.

162 The recyclability of the catalyst was then studied under the optimum conditions (150°C, 20 bar
 163 of hydrogen, 1h f reaction). This is a key parameter as in batch liquid phase reactor, catalysts used in
 164 the literature suffer from leaching and from deposition of furanic derivatives on the catalytic sites
 165 preventing the reuse of the catalyst. The recycling of the catalyst was performed by recovering the
 166 solid owing to its magnetic properties. It was then reused without any treatment. The amount of
 167 furfural used was always 1g for each cycle in 9g of ethanol. Four cycles were performed under 20 bar
 168 of hydrogen for 1h of reaction at 150°C (Figure 3).

169



170
 171

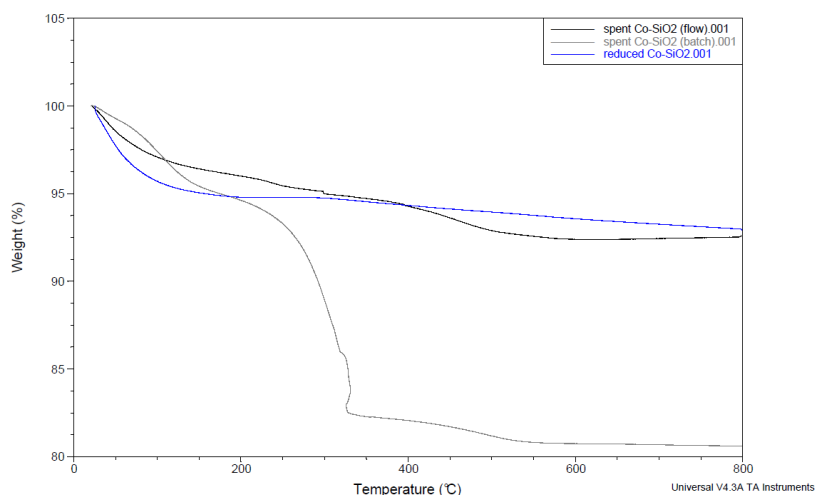
172 **Figure 3.** Recycling of Co/SiO₂. 1g of furfural, 9g of ethanol, T = 150°C, 20 bar of hydrogen, 1h of
 173 reaction.

174

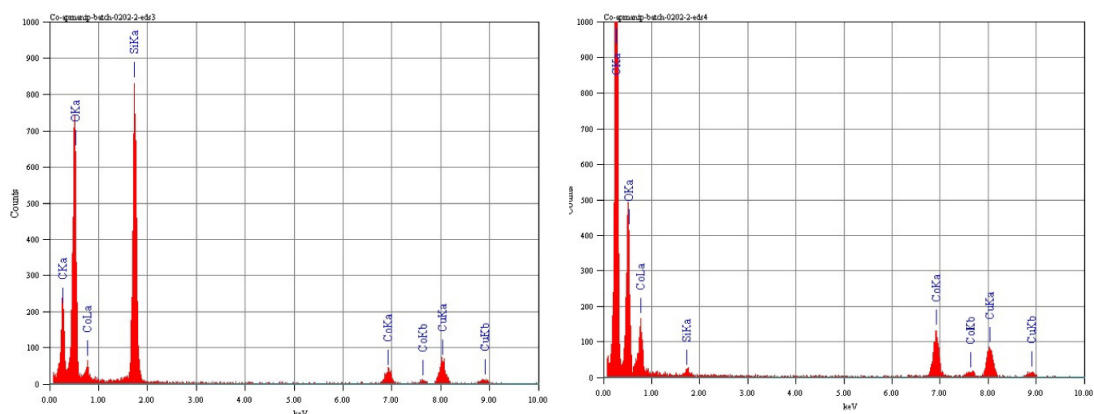
175 FOL selectivity and conversion of furfural slightly decreased after the third cycle, which can be
 176 ascribed to the work up process. However, after the fourth cycle the conversion of furfural dropped
 177 from 100 to 69% and the selectivity to FOL decreased also (88%). This can be due to the poisoning of
 178 cobalt in the solution as it is already mentioned in the literature or to the leaching of cobalt [24, 26]
 179 leading to the formation of by-products such as THFA and other unidentified by-products. To

180 confirm these hypotheses, TGA analysis of the spent catalyst were performed and compared to the
 181 TGA analysis of the fresh catalyst (Figure 4).

182 It was shown that 18% of weight was lost during the TGA analysis of the spent catalyst whereas
 183 only 7% was lost during the fresh catalyst analysis. This increase of the weight loss can be due to the
 184 deposition of carbon species on the catalyst due to the sorption of furanic compounds. To confirm
 185 this hypothesis MET analysis of the spent catalyst was performed (Figure 5).
 186



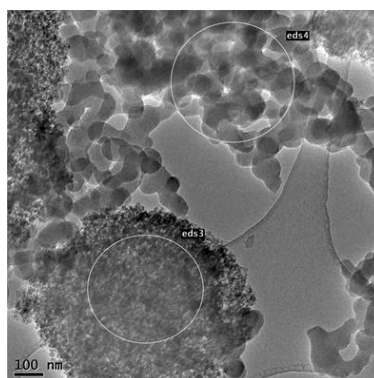
187 **Figure 4.** TGA analysis of the reduced Co/SiO₂ catalyst before reaction and after reaction under batch and
 188 flow conditions.
 189



190

EDS 3

EDS 4



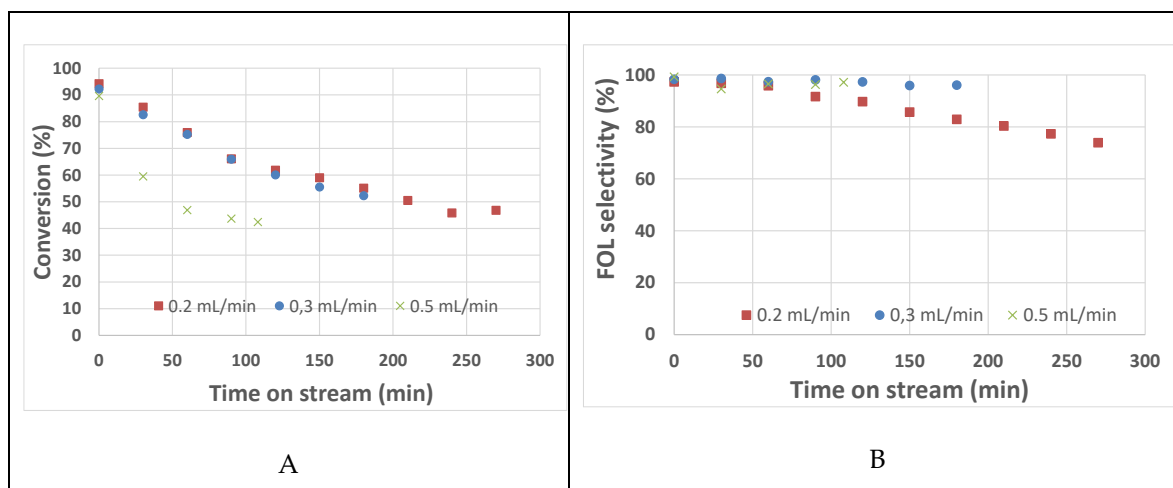
191
 192

Figure 5. TEM images recorded for reduced Co/SiO₂ catalyst after reaction under batch reaction and EDS analysis.

193 It was clearly shown by EDS that carbon was deposited on the catalyst surface leading to less
 194 accessibility of furfural to active sites and a decrease of the selectivity to FOL. Several zones of the
 195 catalyst contain carbon deposit. In order to prevent this deactivation, hydrogenation of furfural was
 196 performed in continuous flow reactor.

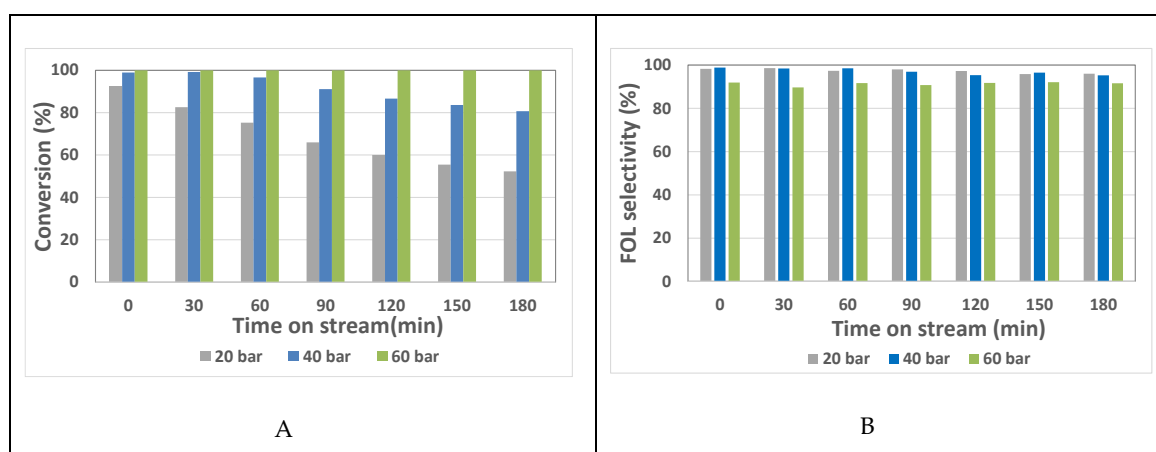
197 3.3. Continuous flow reactor

198 The hydrogenation of furfural was performed while keeping the concentration of furfural used
 199 for batch experiments (5g of furfural in 45 g of ethanol) and the catalyst amount of 260 mg to fill the
 200 catalyst cartridge. In a first set of experiments, the flow rate of the alcoholic solution of furfural was
 201 studied. To this aim, the flow rate was increased from 0.2 to 0.5 mL.min⁻¹ (Figure 6).



202 **Figure 6.** Effect of the alcoholic furfural solution (5g of furfural in 45g of ethanol) flow rate. 150
 203 °C, 20 bar of hydrogen in the presence of 260 mg of Co/SiO₂. (A) conversion vs. TOS. (B) FOL
 204 selectivity vs. TOS.

205 When the flow rate of the furfural solution increased from 0.2 to 0.3 mL min⁻¹, similar trend in
 206 the conversion of furfural was obtained, a drop of the conversion from 94% to 50% being observed in
 207 the function of TOS (Time On Stream) from 0 to 180 min. The selectivity was maintained at around
 208 97% for 0.3 mL.min⁻¹ whereas under 0.2 mL.min⁻¹ of furfural solution, the selectivity to FOL decreased
 209 from 97 to 74%, which is due to the increase of residence time that favored the formation of THFA.



210 **Figure 7.** Effect of the hydrogen pressure. 5 g of furfural in 45 g of ethanol at 0.3 mL. min⁻¹ flow
 211 rate. 150 °C in the presence of 260 mg of Co/SiO₂. (A) conversion vs. TOS. (B) FOL selectivity vs. TOS.

212
 213

214 A further increase of the furfural solution flow rate up to 0.5 mL.min⁻¹ led to a significant drop of
 215 furfural conversion from 90% to 40% after 110 min of reaction. The FOL selectivity was kept constant.

216 Based on these results, it was decided to keep the flow rate of 0.3 mL min⁻¹ for the following
 217 experiments. The effect of the pressure of hydrogen was then studied from 20 to 60 bar (Figure 7).
 218 Increasing the pressure of hydrogen led to an increase of the conversion of furfural from 92 to 100%.
 219 It was interesting to see that under 60 bar of hydrogen the conversion was always 100% when TOS
 220 increased up to 180 min whereas at lower pressure a slight decrease of the conversion was observed.
 221 Concerning the selectivity, it was kept constant independently of the hydrogen pressure but the
 222 selectivity to FOL was lower under 60 bar of hydrogen, due to the formation of THFA as a by-
 223 products. This can be explained by a higher solubility of hydrogen due to its pressure as previously
 224 shown in batch reactions.

225 4. Discussion-Conclusion

226 Hydrogenation of furfural to FOL in a batch reactor in the presence of Co/SiO₂ catalyst is efficient
 227 at 150°C under 20 bar of hydrogen using a solution of furfural of 10 wt.% in ethanol. However, the
 228 stability of the catalyst is not optimal as it is shown by the catalyst recycling. TGA and MET analysis
 229 showed that carbon was adsorbed on the catalyst surface due to the sorption of furanic molecules in
 230 batch reactions as it is already mentioned in the literature [28]. The recyclability of the catalyst was
 231 thus hampered by this coke formation on the catalyst surface.

232 The hydrogenation of furfural to FOL in a continuous flow reactor can afford a high conversion
 233 of furfural with a selectivity higher than 90% under 60 bar of hydrogen at 150°C. It means that the
 234 catalyst was not poisoned when a hydrogen pressure of 60 bar was used but the selectivity was
 235 slightly lower due to further hydrogenation to THFA. At an industrial point of view, it can be
 236 interesting to see the space time yield of the reaction (Table 2). The space time yield (STY) was
 237 calculated and it was higher if the hydrogenation of furfural was performed in a continuous flow
 238 reactor than in a batch reactor. Thus, under similar conditions of pressure and temperature, the STY
 239 was 13.2 g.L⁻¹.h⁻¹ for batch reaction versus 16.6 g.L⁻¹.h⁻¹ for continuous flow reaction. By increasing the
 240 hydrogen pressure, the STY increased in continuous flow reaction from 16.6 to 30.6 g.L⁻¹.h⁻¹. These
 241 results show that using a same catalyst, the hydrogenation of furfural to FOL is more performant in
 242 continuous flow reactor than in batch reactor.

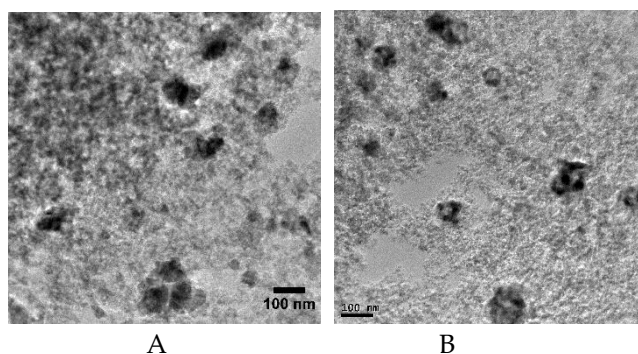
243 **Table 3.** Hydrogenation of furfural: effect of the reactor¹.

Reactor	P _{H2} (bar)	Conversion (%)	Selectivity to FOL (%)	STY (g.L ⁻¹ .h ⁻¹)
Batch ²	20	100	100	13.2
	20	52	50	16.6
Flow ³	40	81	77	26.6
	60	100	92	30.6

244 ¹ furfural in ethanol 10wt.%, Co/SiO₂ = 5 wt% of furfural solution, 150°C. ² reaction time = 1h. ³ time on stream
 245 = 3h; flow rate of alcoholic solution of furfural = 0.3 mL.min⁻¹

246 In order to go deeply in this comparison from these two processes, it was interesting to compare
 247 the stability of the catalyst. In batch reactor, the catalyst was recyclable up to 3 times and lost its
 248 activity but the selectivity was kept constant. This was due to an adsorption of the furanic molecules
 249 on the catalyst surface. For the continuous flow reactor, TGA analysis was performed on the spent
 250 catalyst and only a slight difference in the weight loss was observed between the fresh and the spent
 251 catalyst (Figure 4). The specific surface area was similar before and after reaction. ICP analysis of
 252 spent catalyst showed that there was no leaching of cobalt (9 wt. % before and after reaction). TEM
 253 showed that the particle size did not change after reaction and that no carbon was formed on the
 254 catalyst surface (Figure 8).

255



256

257 **Figure 8.** TEM images recorded for Co/SiO₂ catalyst before (A) and after reaction (B) under continuous flow.

258 The difference of the two processes is the sorption of furanic compounds on the catalyst. In batch
259 processes the catalysts is in contact with the reactant and the products formed which led to a higher
260 contact time between the furanic molecules and the catalysts than in continuous flow process. With
261 these results, it is clearly demonstrated that the stability of the catalyst is higher under continuous
262 flow processes than under batch processes.

263 In continuous flow reactor, it was interesting to see, that by increasing the hydrogen pressure it
264 was possible to maintain the activity of the catalyst for at least 3h and that the selectivity was kept
265 constant above 90%. This can be due to an increase of the hydrogen solubility which is also observed
266 during the hydrogenation in batch reactor, since FOL produced is then hydrogenated to THFA with
267 an increase of the hydrogen pressure from 20 to 40 bar.

268 In conclusion, this study shows that continuous flow reactor can be a solution when a catalyst
269 suffers from a poisoning during batch processes due to sorption of molecules (reactants or products).
270 The optimization of the reaction conditions which are not the same in both processes has to be
271 performed in order to reach similar conversion of furfural and selectivity to FOL.

272

273 **Supplementary Materials:** The following are available online at www.mdpi.com/xxx/s1, Figure S1: title, Table
274 S1: title, Video S1: title.

275 **Author Contributions:** investigation, M.A., D.Z. and Y.W.; supervision, S.R., C.L., K.D.O.V.; writing—K.D.O.V

276 **Funding:** This research was funded by the Poitou-Charentes region for the funding of the PhD grant of Maïté
277 Audemar. ANR agency for the funding of FurCab Project ANR-15-CE07-0016. Région Nouvelle Aquitaine for
278 the funding of this project through the FR CNRS INCREASE 3707, the chaire TECHNOGREEN and FEDER, the
279 University of Poitiers and the CNRS for their financial support. China Scholarship Council (CSC).

280 **Acknowledgments:** In this section you can acknowledge any support given which is not covered by the author
281 contribution or funding sections. This may include administrative and technical support, or donations in kind
282 (e.g., materials used for experiments).

283 **Conflicts of Interest:** The authors declare no conflict of interest. The funders had no role in the design of the
284 study; in the collection, analyses, or interpretation of data; in the writing of the manuscript, or in the decision to
285 publish the results.

286 References

287 References must be numbered in order of appearance in the text (including citations in tables and legends)
288 and listed individually at the end of the manuscript. We recommend preparing the references with a
289 bibliography software package, such as EndNote, ReferenceManager or Zotero to avoid typing mistakes
290 and duplicated references. Include the digital object identifier (DOI) for all references where available.

291
292
293
294
295
296
297
298
299
300
301
302
303
304
305
306
307
308
309
310
311
312
313
314
315
316
317
318
319
320
321
322
323
324
325
326
327
328
329
330
331
332
333
334
335
336
337
338
339
340
341
342
343
344

Citations and References in Supplementary files are permitted provided that they also appear in the reference list here.

In the text, reference numbers should be placed in square brackets [], and placed before the punctuation; for example [1], [1–3] or [1,3]. For embedded citations in the text with pagination, use both parentheses and brackets to indicate the reference number and page numbers; for example [5] (p. 10), or [6] (pp. 101–105).

1. Espro, C.; Gumina, B.; Szumelda, T.; Paone, E.; Mauriello, F. Catalytic Transfer Hydrogenolysis as an effective tool for the reductive upgrading of cellulose, hemicellulose, lignin, and their derived molecules. *Catalysts* **2018**, *8*, 313. doi.org/10.3390/catal8080313
2. Mariscal, R.; Maireles-Torres, P.; Ojeda, M.; Sádaba, I.; López Granados, M. Furfural: A renewable and versatile platform molecule for the synthesis of chemicals and fuels. *Energy Environ. Sci.* **2016**, *9*, 1144–1189. DOI 10.1039/C5EE02666K
3. Bonacci, S.; Nardi, M.; Costanzo, P.; De Nino, A.; Di Gioia, M.; Oliverio, M.; Procopio, A. Montmorillonite K10-Catalyzed Solvent-Free Conversion of Furfural into Cyclopentenones. *Catalysts* **2019**, *9*, 301. doi.org/10.3390/catal9030301
4. Smirnov, A.; Selishcheva, S.; Yakovlev, V. Acetalization Catalysts for Synthesis of Valuable Oxygenated Fuel Additives from Glycerol. *Catalysts* **2018**, *8*, 595. https://doi.org/10.3390/catal8120595
5. Morozov, E. Furfural Production, 2nd ed.; Forest Industry: Moscow, Russia, 1988; pp. 32–56.
6. Liu, D.; Zemlyanov, D.; Wu, T.; Lobo-Lapidus, R.J.; Dumesic, J.A.; Miller, J.T.; Marshall, C.L. Deactivation mechanistic studies of copper chromite catalyst for selective hydrogenation of 2-furfuraldehyde. *J. Catal.* **2013**, *299*, 336–345. https://doi.org/10.1016/j.jcat.2012.10.026
7. Musci, J.J.; Merlo, A.B.; Casella, M.L. Aqueous phase hydrogenation of furfural using carbon-supported Ru and RuSn catalysts. *Catal. Today* **2017**, *296*, 43–50. https://doi.org/10.1016/j.cattod.2017.04.063
8. Vorotnikov, V.; Mpourmpakis, G.; Vlachos, D.G. DFT study of furfural conversion to furan, furfuryl alcohol, and 2-methylfuran on Pd(111). *ACS Catal.* **2012**, *2*, 2496–2504. https://doi.org/10.1021/cs300395a
9. Vaidya, P.D.; Mahajani, V.V. Kinetics of Liquid-Phase Hydrogenation of Furfuraldehyde to Furfuryl Alcohol over a Pt/C Catalyst. *Ind. Eng. Chem. Resour.* **2003**, *42*, 3881–3885. https://doi.org/10.1021/ie030055k
10. Zhao, Y. Facile synthesis of Pd nanoparticles on SiO₂ for hydrogenation of biomass-derived furfural. *Environ. Chem. Lett.* **2014**, *12*, 185–190. https://doi.org/10.1007/s10311-013-0432-4
11. Mironenko, R.M.; Belskaya, O.B.; Gulyaeva, T.I.; Nizovskii, A.I.; Kalinkin, A.V.; Bukhtiyarov, V.I.; Lavrenov, A.V.; Likholobov, V.A. Effect of the nature of carbon support on the formation of active sites in Pd/C and Ru/C catalysts for hydrogenation of furfural. *Catal. Today* **2015**, *249*, 145–152. https://doi.org/10.1016/j.cattod.2014.10.037.
12. Fulajtárova, K.; Soták, T.; Hronec, M.; Vávra, I.; Dobročka, E.; Omastová, M. Aqueous phase hydrogenation of furfural to furfuryl alcohol over Pd–Cu catalysts. *Appl. Catal. A* **2015**, *502*, 78–85. https://doi.org/10.1016/j.apcata.2015.05.031
13. Wu, J.; Shen, Y.; Liu, C.; Wang, H.; Geng, C.; Zhang, Z. Vapor phase hydrogenation of furfural to furfuryl alcohol over environmentally friendly Cu–Ca/SiO₂ catalyst. *Catal. Commun.* **2005**, *6*, 633–637. https://doi.org/10.1016/j.catcom.2005.06.009
14. Villaverde, M.M.; Bertero, N.M.; Garetto, T.F.; Marchi, A.J. Selective liquid-phase hydrogenation of furfural to furfuryl alcohol over Cu-based catalysts. *Catal. Today* **2013**, *213*, 87–92. https://doi.org/10.1016/j.cattod.2013.02.031
15. Khromova, S.A.; Bykova, M.V.; Bulavchenko, O.A.; Ermakov, D.Y.; Saraev, A.A.; Kaichev, V.V.; Venderbosch, R.H.; Yakovlev, V.A. Furfural Hydrogenation to Furfuryl Alcohol over Bimetallic Ni–Cu Sol–Gel Catalyst: A Model Reaction for Conversion of Oxygenates in Pyrolysis Liquids. *Top. Catal.* **2016**, *59*, 1413–1423. https://doi.org/10.1007/s11244-016-0649-0
16. Sitthisa, S.; Sooknoi, T.; Ma, Y.; Balbuena, P.B.; Resasco, D.E. Kinetics and mechanism of hydrogenation of furfural on Cu/SiO₂ catalysts. *J. Catal.* **2011**, *277*, 1–13. https://doi.org/10.1016/j.jcat.2010.10.005
17. Smirnov, A.A.; Shilov, I.N.; Alekseeva, M.V.; Selishcheva, S.A.; Yakovlev, V.A. Study of the Composition Effect of Molybdenum-Modified Nickel–Copper Catalysts on Their Activity and Selectivity in the Hydrogenation of Furfural to Different Valuable Chemicals. *Catal. Ind.* **2018**, *10*, 228–236. DOI: 10.1134/S2070050418030091

- 345 18. Audemar M., Ciotonea, C., K. De Oliveira Vigier, S. Royer, A. Ungureanu, B. Dragoi, E. Dumitriu, F.
346 Jérôme. Selective Hydrogenation of Furfural to Furfuryl Alcohol in the Presence of a Recyclable
347 Cobalt/SBA-15 Catalyst. *ChemSusChem* 2015, 8, 1885-1891. <https://doi.org/10.1002/cssc.201403398>
- 348 19. Villaverde, M.M.; Garetto, T.F.; Marchi, A.J. Liquid-phase transfer hydrogenation of furfural to furfuryl
349 alcohol on Cu–Mg–Al catalysts. *Catal. Commun.* 2015, 58, 6–10. <https://doi.org/10.1016/j.catcom.2014.08.021>
- 350 20. Srivastava, S.; Mohanty, P.; Parikh, J.K.; Dalai, A.K.; Amritphale, S.S.; Khare, A.K. Cr-free Co–Cu/SBA-15
351 catalysts for hydrogenation of biomass-derived α -, β -unsaturated aldehyde to alcohol. *Chin. J. Catal.* 2015,
352 36, 933–942. [https://doi.org/10.1016/S1872-2067\(15\)60870-1](https://doi.org/10.1016/S1872-2067(15)60870-1)
- 353 21. Wei, S.; Cui, H.; Wang, J.; Zhuo, S.; Yi, W.; Wang, L.; Li, Z. Preparation and activity evaluation of NiMoB/-
354 Al₂O₃ catalyst by liquid-phase furfural hydrogenation. *Particuology* 2011, 9, 69–74.
355 <https://doi.org/10.1016/j.partic.2010.05.009>
- 356 22. Garcia-Olmo, J.; Yepez, A.; Balu, A. M.; Prinsen, P.; Garcia, A.; Mazière, A.; Len, C.; Luque, R.
357 Activity of continuous flow synthesized Pd-based nanocatalysts in the flow hydroconversion of furfural.
358 *Tetrahedron* 2017, 73, 5599-5604. <https://doi.org/10.1016/j.tet.2017.02.056>
- 359 23. Wang, Y.; Prinsen, P.; Triantafyllidis, K.S.; Karakoulia, S.A.; Yepez, A.; Len, C.; Luque, R.; Batch vs
360 continuous flow performance of supported mono- and bimetallic nickel catalysts for catalytic transfer
361 hydrogenation of furfural in isopropanol. *ChemCatChem.* 2018, 10, 3459-3468.
362 <https://doi.org/10.1002/cctc.201800530>
- 363 24. Wang, Y.; Prinsen, P.; Triantafyllidis, K.S.; Karakoulia, S.A.; Trikalitis, P.N.; Yepez, A.; Len, C.; Luque, R.
364 Comparative study of supported monometallic catalysts in the liquid-phase hydrogenation of furfural :
365 batch and continuous flow. *ACS Sustainable Chem. Eng.* 2018, 6, 9831-9844.
366 <https://doi.org/10.1021/acssuschemeng.8b00984>
- 367 25. Selishcheva, S. A.; Smirnov, A. A.; Fedorov, A. V., Ermakov, D. Yu., Gulyaeva, Yu. K., Yakovlev, V. A.
368 Production of Furfuryl Alcohol in the Presence of Copper-Containing Catalysts in the Selective
369 Hydrogenation of Furfural. *Catalysis in Industry* 2019, 11, 216–223. doi: 10.1134/S2070050419030103
- 370 26. Wang, Y.; Deyang, P.; Rodriguez-Pradrón, D.; Len, C. Recent Advances in Catalytic Hydrogenation
371 of Furfural. *Catalysts* 2019, 9, 796; doi:10.3390/catal9100796.
- 372 27. Audemar, M.; Ramdani, W., Junhui, T.; Ifrim, A.R.; Ungureanu, A.; Jérôme, F.; Royer, S.; De Oliveira
373 Vigier, K. Selective hydrogenation of xylose to xylitol over Co/SiO₂ catalysts. *ChemCatChem* 2020,
374 <https://doi.org/10.1002/cctc.201901981>
- 375 28. Taylor, M.J.; Jiang, L.; Reichert, J.; Papageorgiou, A.C.; Beaumont, S.K.; Wilson, K.; Lee, A.F.; Barth, J.V.;
376 Kyriakou, G. Catalytic Hydrogenation and Hydrodeoxygenation of Furfural over Pt(111): A Model System
377 for the Rational Design and Operation of Practical Biomass Conversion Catalysts. *J Phys Chem C Nanomater*
378 *Interfaces* 2017, 121, 8490–8497. doi: 10.1021/acs.jpcc.7b01744
- 379



© 2019 by the authors. Submitted for possible open access publication under the terms and conditions of the Creative Commons Attribution (CC BY) license (<http://creativecommons.org/licenses/by/4.0/>).